Chapter 02: Literature Survey

2.1 Preamble

The present chapter aims to review and highlight the contribution of various researchers. The first section of this chapter will develop a basic understanding of the stir casting process. Along with this, several characteristics of stir cast composites and the effect of process parameters on microstructure, mechanical and tribological properties of stir cast composites have been discussed. The second section of the chapter discusses the work accomplished in the field of Friction Stir Processing (FSP). The second section focuses on variation in microstructure, mechanical and tribological properties as a result of varying rotational speed, transverse speed, axial load and tool tilt angle. Lastly, the third section discusses the work done in the field of Friction Stir Welding (FSW). The section reviews the work related to macrostructure and microstructure of welded composites along with mechanical properties, wear and corrosive properties.

2.2 Manufacturing of AMC using Stir Casting Process

There exist several casting processes using which Aluminium Matrix Composites (AMC) can be manufactured. Among these techniques, centrifugal casting and stir casting are the most frequently implemented techniques. It should be noted that the centrifugal casting process has several limitations such as fabrication of only cylindrical shapes i.e. disc, rings or pipe like structures. Thus, to avoid the aforementioned drawbacks, the stir casting process can be adopted. The stir casting process is capable of fabricating composites having complex shapes. Comparison carried out by researchers revealed that the stir casting is better in every aspect compared to several processes under the action of centrifugal force (Taha, 2001; Surappa, 1997). This casting process is feasible for industrial purposes as it manufactures composite at a comparatively lower cost (Soltani, et al., 2017). The dispersal of reinforcement particles into the molten matrix is governed by a mechanical stirrer which is externally driven by the motor placed vertically above it (Sijo & Jayadevan, 2016). It has been reported that the stirring action not only transfers the secondary phase particles into molten matrix but also tends to rearrange them (Hashim, Looney, & Hashmi, 1999; Kumaran, Uthayakumar, Slota, Aravindan, & Zajac, 2016). The reinforcing material is directly added to the vortex

created due to the stirring of the molten matrix. It has been suggested that preheating of reinforcement particles should be carried out so that the humidity/moisture from secondary phase particles gets removed (Ravi, Naik, & Prakash, 2015; Sijo & Jayadevan, 2016). Also, preheating will avoid thermal mismatch occurred during the addition of reinforcement particles into the molten matrix (Yu, Qiu-lin, Dong, Wei, & U., 2016).

The various parameters governing the distribution of reinforcement particles are stirrer design (Sajjadi, Ezatpour, & Beygi, 2011), the rotational speed of stirrer (Moses & Sekhar, 2016), blade angle of the stirrer, melting temperature, holding temperature (Agarwala & Dixit, 1981), stirring time and stirrer position (Naher, Brabazon, & Looney, 2003). Mollaei et al. (2018) manufactured Al/SiO_2 nano-composites and investigated the variation in microstructure, mechanical and tribological properties by varying pouring temperature and stirring time. A comparative study between reinforced composite and aluminium alloy was also reported. Initially, Al-Si alloy and SiO_2 nano-particles powder were mixed in presence of argon gas using a planetary ball mill machine. Then, this prepared mixture was heated in the furnace and reinforcement powders were added to the molten matrix. It was observed that by using powders, agglomeration in microstructure was less than 100 μm. On the addition of SiO_2 nano-particles in the molten matrix at higher temperature i.e. 800 - 850 °C, enhancement in amount and size of Al-Ni intermetallic phase was reported. Due to the same, the mechanical properties of those composites were higher. Enhancement in wear resistance, hardness and elastic modulus was reported due to the homogenous distribution of SiO_2 nano-particles. Reduction in porosity was observed when nano-composites were manufactured by maintaining pouring temperature at 750 °C and varying the stirring time from 2 min to 4 min. Khademian et al. (2016) also investigated the variation in microstructure and mechanical properties of A356/B_4C composites by varying pouring temperature and stirring time. The variation in tensile strength with the change in pouring temperature and stirring time is shown in Figure 2.1. It can be observed that for constant pouring time, an increase in pouring temperature initially tends to enhance mechanical properties. However, after a specific point, an increase in pouring temperature was found to degrade the mechanical properties. A similar trend was observed for constant pouring temperature and varying stirring time. Optimum results were observed for specimens manufacture at a pouring temperature of 850 °C and stirring time of 15 minutes. Optical microscopy images of composites manufactured by maintaining stirring time as 15 minutes and varying pouring

temperature is shown in Figure 2.2. While comparing Figure 2.2(a) and Figure 2.2(b), it can be observed that increase in pouring temperature from 850 °C to 950 °C leads to grain refinement. Also with higher pouring temperature, formation of dendritic structure along with agglomeration of reinforcement particles can be observed. This dendritic structure and agglomerated particles will reduce the mechanical properties of cast composites. The consequence of hot rolling and hot extrusion on mechanical properties of manufactured composites was also investigated (Khademian, Alizadeh, & Abdollahi, 2016). Due to the same, reduction/refinement in size of pores and defects were observed and thus, enhancement in mechanical properties was reported. Furthermore, this deformation process leads to modify the microstructure. The hot rolling and hot extrusion tends to break the clusters of reinforcement particles and leads to homogeneous distribution. On comparing the tensile strength of composite after hot rolling and hot extrusion, a negligible difference was reported. Naher et al. (2003) in their study attempted to optimize process parameters. A mixture of glycerol and water was created so that it mimics the molten aluminium, as the viscosity of this mixture was similar to that of molten aluminium. Particles of SiC were then added to this mixture. It was observed that stirrer or impeller with four or three blades each at an angle of 60° or turbine blade impeller tends to distribute reinforcement particles homogenously.

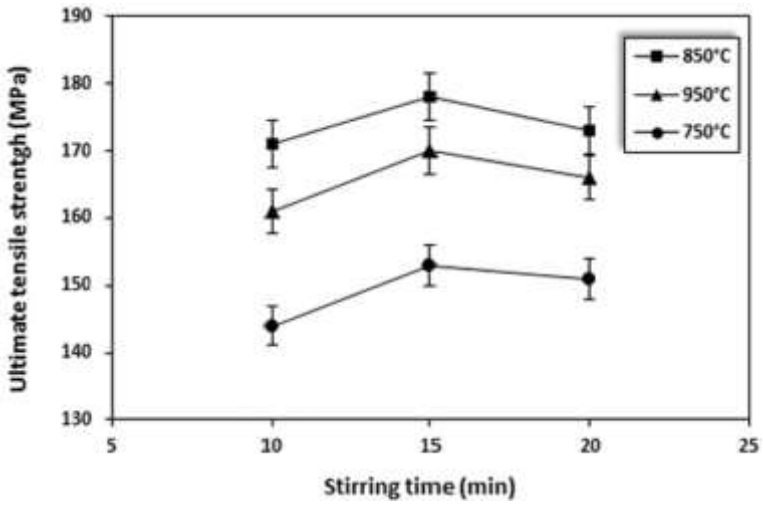

Figure 2.1 Effect of different pouring temperature and stirring time on ultimate tensile strength (Khademian, Alizadeh, & Abdollahi, 2016)

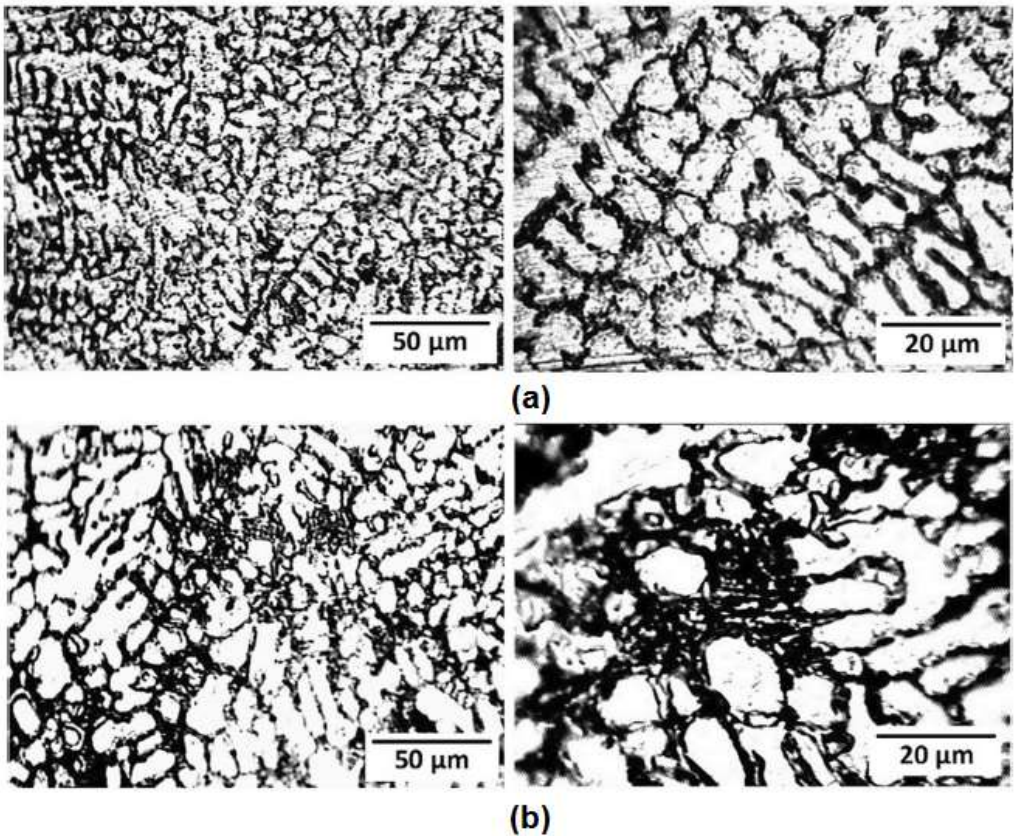

Figure 2.2 Optical Microscopy of As-cast composites constant stirring time of 15 min and (a) pouring temperature 850 °C and (b) pouring temperature 950 °C (Khademian, Alizadeh, & Abdollahi, 2016)

Sozhamannan et al. (2012) from their study reported that melting temperature and holding temperature dominates the wettability and distribution of particles. If the temperature of the melt is higher than the melting point, then the molten matrix will have low viscosity. This lower viscosity of molten matrix will improve the distribution of secondary phase particles and will also provide better retention (Agarwala & Dixit, 1981; Sozhamannan, Prabu, & Venkatagalapathy, 2012). It was suggested that wettability between molten matrix and reinforcement particles can be improved by removing the gas layer from the top surface (Ezatpour, Sajjadi, Sabzevar, & Huang, 2014). Apart from this, it was also reported that wettability can be improved by providing stirring action such that it overcomes surface tension (Hashim, Looney, & Hashmi, 1999). On the other side, it was also reported that excessive stirring reduces wettability (Naher, Brabazon, & Looney, 2003). Prabu et al. (2006) studied the dispersal pattern of SiC particles in molten aluminium, by varying stirring speed and stirring time. It was also reported that for Al-SiC composite, to obtain the homogenous distribution of SiC particles, stirring speed can

be maintained at 600 rpm for a time period of 10 min. Figure 2.3 represents the hardness distribution for composites fabricated at a constant stirring speed of 600 rpm and varying the stirring time from 5 minutes to 15 minutes. From Figure 2.3, it can be observed that an increase in stirring time from 5 minutes to 10 minutes results in enhancement of hardness. However, no subsequent improvement in hardness was observed for an increase in stirring time beyond 10 min. Similarly, Figure 2.4 represents the variation in hardness by varying stirring speed from 500 rpm to 700 rpm with a constant stirring time of 5 min. Hardness was found to improve with the increase in stirring speed from 500 rpm to 600 rpm. Whereas, reduction in hardness was observed for stirring speed exceeding 600 rpm. For fabrication of Al_2O_3 reinforced Al-Mg composite it was reported that wettability can be improved with stirring speed of 960 rpm, stirrer height of 0.81, stirrer diameter of 0.63 and holding temperature between 605 to 615 °C (Ghosh, Ray, & Rohatgi, 1984).

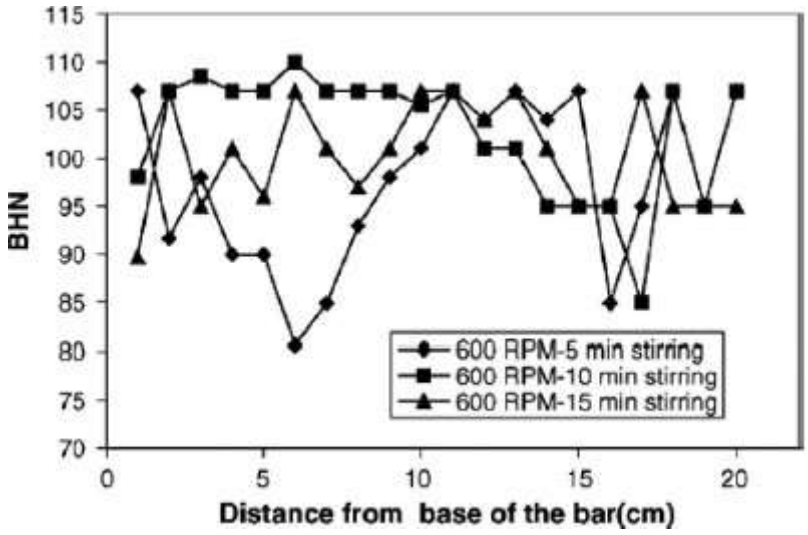

Figure 2.3 Effect of constant stirring speed (600 rpm) and different stirring time on the hardness of Al-SiC composites (Prabu, Karunamoorthy, Kathiresan, & Mohan, 2006)

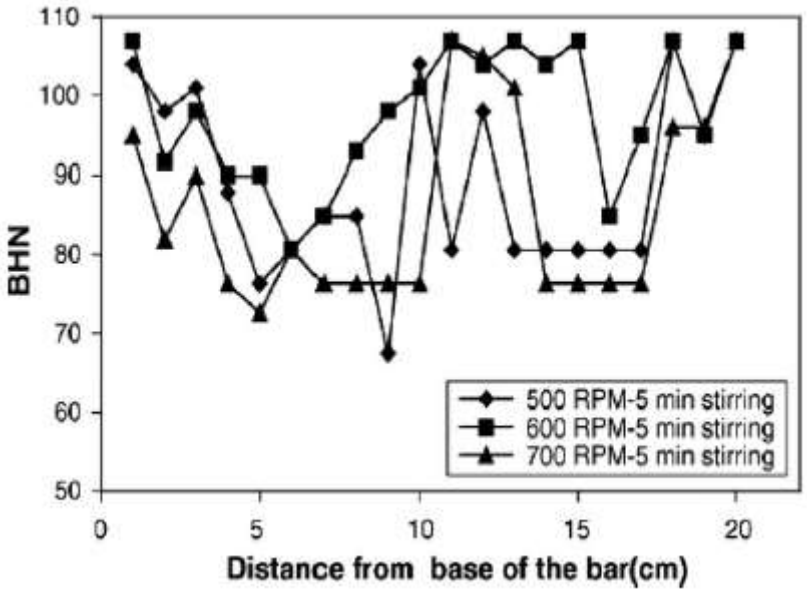

Figure 2.4 Effect of different stirring speed and constant stirring time (5 min) on the hardness of Al-SiC composite (Prabu, Karunamoorthy, Kathiresan, & Mohan, 2006)

Das et al. (2006) examined the consequence of different particles size of zircon sand incorporated in the aluminium matrix. In comparison with finer particles, coarsen particles were found to have a substantial amount of dispersion in the aluminium matrix. Also, it was reported that abrasive wear resistance improves when the volume of particles increases or particles size decreases. Gui et al. (2004) fabricated magnesium based composite using vacuum stir casting process. A comparative study between the microstructure of as-cast composite and heat treated composite was carried out. The microstructure of both i.e. Mg-Al9Zn magnesium alloy and as-cast Mg-Al9Zn/15SiC composite is shown in Figure 2.5. While comparing Figure 2.5 and Figure 2.6, it can be observed that, providing T4 heat treatment leads to homogenous distribution of SiC particles. Literature also represents the used electromagnetic assisted stir casting process for manufacturing of A356/SiC (Dwivedi, Sharma, & Mishra, 2014). The major advantage of this process was that it leads to grain refinement. Along with this, electromagnetic stirring tends to have more homogenously distributed secondary phase particles compared to conventional stir cast composites. As shown in Figure 2.7, the composites fabricated using electromagnetic stir casting was found to have lower porosity. Due to lower porosity, significant improvement in mechanical properties such as tensile strength, hardness, toughness and fatigue strength was reported.

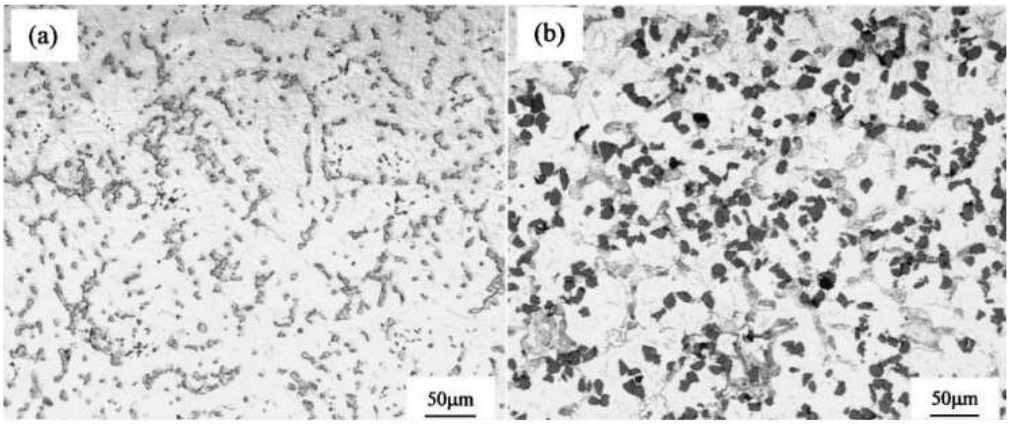

Figure 2.5 Microstructure of (a) Mg-Al9Zn magnesium alloy and (b) as-cast Mg-Al9Zn/15SiC composite (Gui, Han, & Li, 2004)

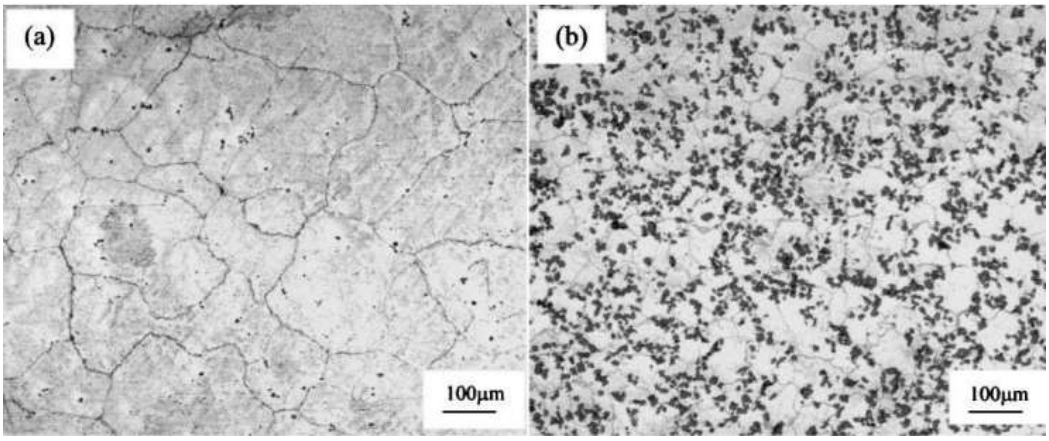

Figure 2.6 Microstructure of T4 treated (a) Mg-Al9Zn magnesium alloy and (b) Mg-Al9Zn/15SiC composite (Gui, Han, & Li, 2004)

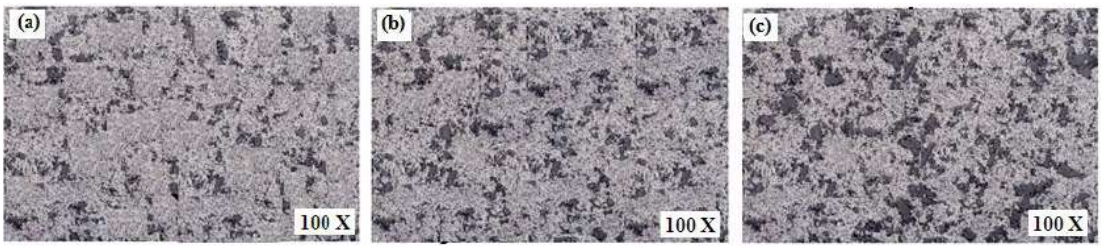

Figure 2.7 Microstructure of A356/SiC composites (a) 5% SiC (b) 10% SiC and (c) 15% SiC (Dwivedi, Sharma, & Mishra, 2014)

Apart from this, two stage stir casting was adopted for manufacturing AA 2014 based MMC reinforced with 9% and 12% of Al_2O_3 (Bharath, Ajawan, Nagaral, Auradi, & Kori, 2018). SEM images of manufactured composites revealed the presence of Al_2O_3

particles which were uniformly distributed within the α-Al matrix. Along with this, defect free microstructure with the presence of few agglomerations of Al_2O_3 particles was observed. In comparison with the ordinary stir casting process, two stage stir casting process tends to improve the dispersal of reinforcement particles in the molten matrix. Also, it was reported that, two stage stir casting process tends to enhance the mechanical and tribological properties of cast composite. From SEM of AA 2014 + ZrO_2 composites manufactured using two stage stir casting process, it was observed that resulting composites was free from casting defects at the microstructural level. Also, the ZrO_2 particles were homogeneously distributed in the aluminium matrix due to which, enhancement in mechanical and tribological properties was reported (Nagaral, Hiremath, Auradi, & Kori, 2018). Al/Al_2O_3 composite was fabricated using the combined effect of the stir casting process and squeeze casting (Sekar, Allesu, & Joseph, 2015). From Figure 2.8, it can be observed that an increase in weight percent of reinforcement particles will result in the formation of agglomeration/clusters. This cluster formation was found to affect the wear properties of manufactured composites. Dry wear studies reveal that composites with 0.5% and 1% of Al_2O_3 were found to have lesser wear loss compared to composites having 1.5% of Al_2O_3.

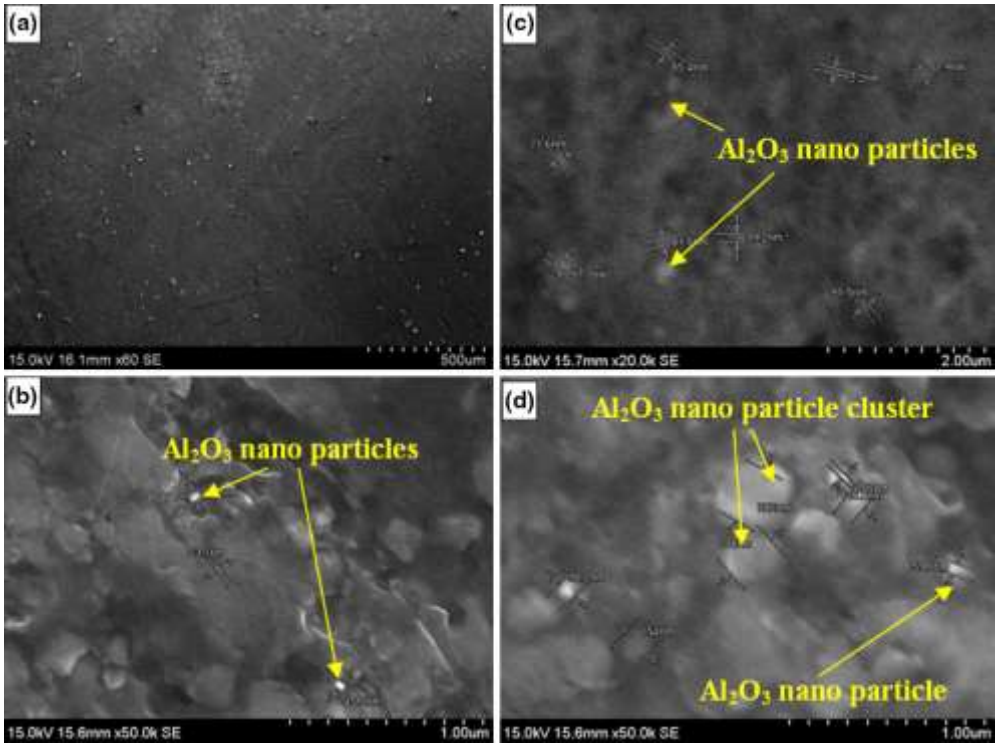

Figure 2.8 SEM images of (a) as-cast A356 alloy (b) A356 + 0.5% Al_2O_3 (c) A356 + 1% Al_2O_3 and (d) A356 + 1.5% Al_2O_3 (Sekar, Allesu, & Joseph, 2015)

The effect of preheating and the addition rate of fly ash in the aluminium alloy were examined. It was reported that porosity and cluster formation can be avoided or reduce by increasing preheat temperature and reducing the rate of addition of fly ash (Juang, Fan, & Yang, 2015). While examining interfacial characteristics of AZ91/SiC, three distinguished types of the interface were observed which were named as Type I, Type II and Type III. For Type I, the interface surface revealed direct contact of interface product with the surface of SiC particles. Whereas, direct contact of interface product with the surface of SiC particles were not observed in type II interface surface. Type III was only found to have two surfaces that were formed as a result of the reaction between matrix and reinforcement (Wang, et al., 2009). It was observed that the bottom pouring setup of stir casting avoids impurities present on the surface of melt and reduces the pouring time (Sekar, Allesu, & Joseph, 2013; Agarwala & Dixit, 1981; Chandrakanth, Rajkumar, & Aravindan, 2010). A novel technique was developed, where the route of stir casting was consisting of a melt-stir-squeeze-bottom pouring setup which leads to the manufacturing of MMC (Singh & Bala, 2017). Composites such as A356/SiC nano-particles, AA 6082/ (Si_3N_4+Gr), AA 2024/B_4C, AA 7075/ (SiC+Al_2O_3), AA 6061/SiC, Aluminium LM4/ Tungsten Carbide (WC), Al/SiC, Al/(SiC+MoS_2) and many more were manufactured using stir casting method. Suthar et al. (2018) critically analyzed the issues such as particles distribution, wettability and porosity faced during manufacturing of composites materials.

Due to the prolonged liquid-reinforcement contact involved in the stir casting process, a considerable amount of interfacial reaction takes place. This interfacial reaction generates several interfacial products which tend to degrade the mechanical properties of stir cast composites. For instance, during the manufacturing of Al-SiC composites, the interfacial reaction between Al and SiC tends to generate the Al_4C_3 phase. This Al_4C_3 phase reacts with moisture present in the atmosphere and ultimately degrades the mechanical properties of composites. However, it should be noted that the formation of deleterious interfacial phase can be controlled by (i) modifying the chemical composition of the matrix, (ii) controlling process parameters of stir casting and (iii) surface modification of reinforcement by coating or passive oxidization (Suthar & Patel, 2018; Shorowordi, Laoui, Haseeb, Celis, & Froyen, 2003; Pech-Canul, 2000). It has been reported that the presence of silicon plays a crucial role in the enhancement of several characteristics of Al/SiC composites. The presence of silicon as alloying element retards

the kinetics of chemical reaction that leads to the formation of the unwanted phase of Al_4C_3 and Al_4SiC_4.

The stir casting process deals with two different materials which are mixed together. One of the material will remain in molten state (matrix material), whereas the other material will be in solid state (reinforcement particles). Both the considered material tends to have different characteristics and behave differently at temperature maintained during stir casting process (Sankhla & Patel, 2021). It should be noted that this difference in characteristics of matrix and reinforcement will affect the wettability and results in generation of intermetallic compounds. The means to avoid intermetallic compounds and enhance wettability has already been discussed earlier. Apart from this, the differences in characteristics of matrix and reinforcement material promote casting defects. Voids and Porosity are the most commonly observed defects in stir cast composites (Aqida, Ghazali, & Hashim, 2012; Ahmad, Hashim, & Ghazali, 2007). The presences of these defects in cast composites leads to failure from pores, reduction in ductility and thus affect several mechanical, tribological and corrosive properties (Yigezu, Jha, & Mahapatra, 2013). Two primary reason for formation of porosity are (1) formation of gas envelop around reinforcement particles and (2) entrapment of gas during stirring. Other than these, factors such as presence of water vapor on reinforcement particles, hydrogen evolution, vigorous stirring and shrinkage during solidification may result in porosity. Lastly, the selection of process parameters such as stirring time, holding time, stirring speed, position of impeller becomes necessary to avoid the formation of porosity. The addition of SiC particles in the form of Al/SiC powder and casting in a semi-solid state was proven beneficial. By doing do, the hardness of the cast composites was increased by 10% and porosity was reduced by 68% (Mortensen & Jin, 1992). Apart from this, use of smaller size of reinforcement particle will also reduce porosity. This will result in greater mismatch in coefficient of thermal expansion of matrix and reinforcement at particle/matrix interface which will increase the dislocation density (Galarraga, Lados, Dehoff, Kirka, & Nandwana, 2016). Apart from this, it has been reported that pre-heating of mould tends to reduce the possibility of casting defects (Prabu, Karunamoorthy, Kathiresan, & Mohan, 2006; Moses & Sekhar, 2016). Lastly, there exist several techniques such as extensive inert gas bubbling through melt, compo-casting in vacuum, casting under pressure, compression and extradition of cast composites, rolling of cast composite and degassing liquid aluminium alloy which tends to reduce the defects in

manufactured composites (Hashim, Looney, & Hashmi, 1999; Ahlatci, Kocer, Candan, & Cimenog lu, 2006).

2.2 Processing of Composites using Friction Stir Processing

The characteristics of resulting surface composites depends upon certain processing parameters such as the design of tool pin, dimension of tool shoulder, tool rotational speed, tool transverse speed, type of tool, size and weight/volume percent of reinforcement particles, number of passes and many more. Not only the microstructure, but these process parameters also affect the mechanical properties, corrosion properties and wear properties of resulting surface composites. From existing literature, it can be observed that commonly used alloys for the matrix phase are aluminium, magnesium and copper, whereas there exist a wide variety of secondary phase reinforcement particles. Dinaharan (2016) investigated the change in microstructure and mechanical properties of surface composites by varying ceramic particles. AA 6082 was used as matrix phase and considered reinforcement particles were Silicon Carbide (SiC), Aluminium Oxide (Al_2O_3), Titanium Carbide (TiC), Boron Carbide (B_4C) and Tungsten Carbide (WC). Investigation of microstructure and mechanical properties of various surface composites reported negligible variation in grain size, tensile strength and hardness. From Figure 2.9 it can be observed that the stirring action of the rotating tool leads to refinement of reinforcement particle. However, maximum tensile strength and hardness were observed for the AA 6082/TiC composite. It was reported that irrelevant to the type of ceramic particles, the microstructure of all surface composites showed the homogeneous distribution of reinforcement particles. At the same time, no interfacial reaction between matrix and different reinforcement particles was reported. Due to the same, enhanced mechanical properties along with good interfacial bonding between matrix and reinforcement particles was observed. Also due to the addition of several types of ceramic particles, fracture mode was found to shift from ductile to brittle.

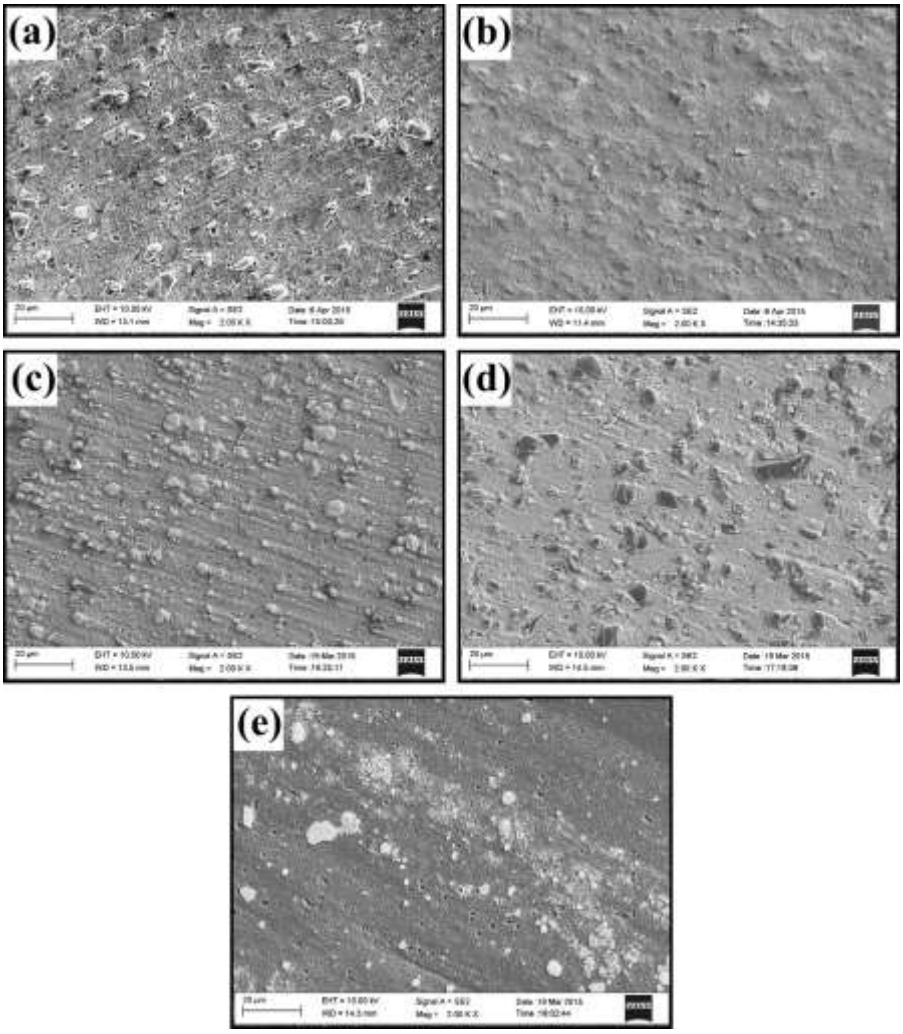

Figure 2.9 Microstructure of AA 6082 reinforced with (a) SiC (b) Al_2O_3 (c) TiC (d) B_4C (e) WC (Dinaharan, 2016)

Kurt (2016) fabricated aluminium based MMC and investigated variation in tensile strength in the light of process parameters and hybrid ratio. Considered process parameters were rotational speed, transverse speed and volume percent of different reinforcement particles. Surface composites were prepared by reinforcing AA 5083 with different reinforcement particles such as SiC, Al_2O_3, Carbon Nanotube (CNT), Graphite (Gr), Zirconium Oxide (ZrO_2). Using these reinforcement phases, hybrid surface composites were manufactured. It was reported that an increase in the volume of CNT, tool rotational speed and transverse speed ultimately improves the tensile strength of surface composites. Among hybrid composites, maximum tensile strength was obtained for AA 5083/10% Gr + 5% ZrO_2. It was reported that increasing tool rotational speed and transverse speed leads to refinement of reinforcement particles. Due to this refinement,

improvement in mechanical properties was reported. Narimani et al. (2016) manufactured mono and hybrid surface composites of AA 6063 and investigated the consequence of weight percent of reinforcement particles on microstructure and wear properties. Different types of aluminium based surface composites were fabricated by incorporating milled B_4C and in-situ TiB_2. Similar to other literature, the microstructure was characterized by homogenously distributed reinforcement particles. Across the cross-section of manufactured composites, improvement in hardness was observed when the weight percent of reinforcement particles was increased. Results of pin-on-disc sliding wear test revealed that with the improvement in hardness, the wear rate of composites was decreasing. Superior hardness and wear resistance were observed for the sample consisting of 100% of TiB_2. Variation in hardness profile across the width of the cross-section is represented in Figure 2.10. Also, variation in wear rate with the variation in proportion of secondary phase particles is shown in Figure 2.11. Characteristic of ceramic particles are higher hardness and better wear resistance. The addition of ceramic particles in matrix tends to enhance the hardness and wear resistance of surface composites. Also, enhancement in hardness is attributed to two facts: (1) FPS leads to grain refinement which ultimately improves hardness and (2) temperature rise during FSP results in annealing of material. Du et al. (2016) also observed the superior hardness and tensile strength when AA 6061 was reinforced with both Al_2O_3 and CNT.

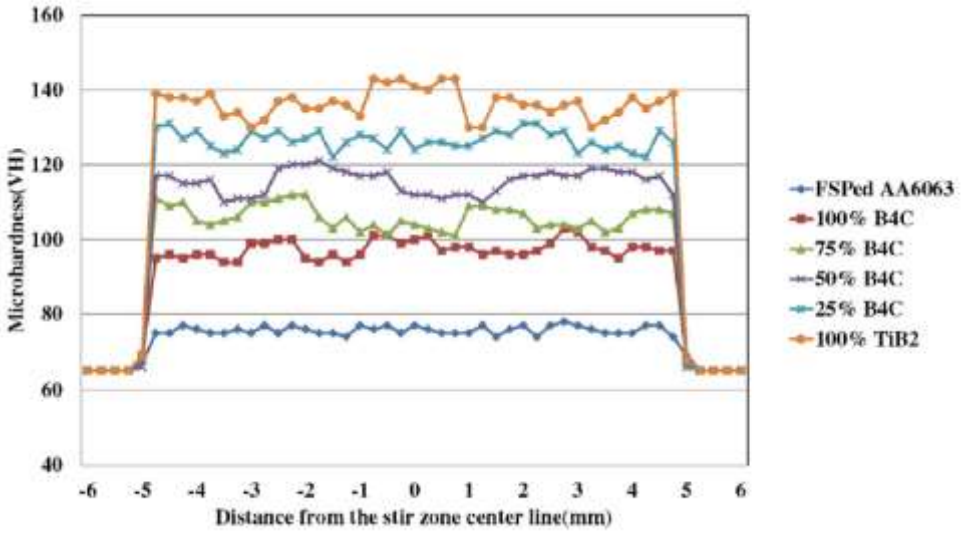

Figure 2.10 Hardness profile for AA 6063 based surface composite with a different weight percent of reinforcement particles (Narimani, Lotfi, & Sadeghian, 2016)

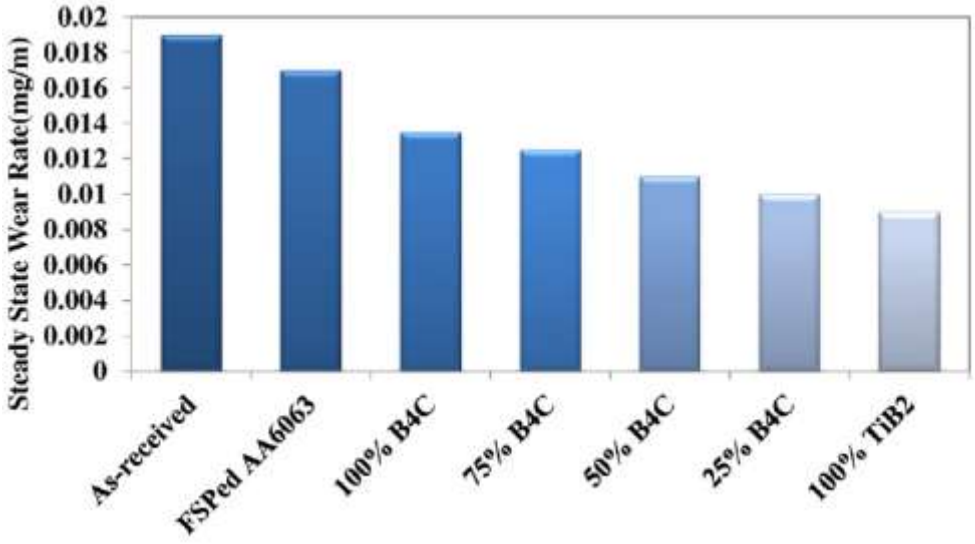

Figure 2.11 Results of wear rate of AA 6063 surface composite with different weight percentage of reinforcement particles (Narimani, Lotfi, & Sadeghian, 2016)

Dinaharan et al. (2016) used fly ash (a waste product from burnt coal) as reinforcement particles in AA 6061 to manufacture surface composite. By the addition of fly ash to the aluminium matrix, improvement in hardness as well as wear resistance was reported. Rathee et al. (2017) investigated the variation in microstructure and mechanical properties with changing ratio of groove width to tool shoulder diameter. Five different samples were considered with a different groove width, constant shoulder diameter and optimized process parameters. An increase in groove width from 0 to 3 mm or 40% volume of reinforcement particles, consequently improves the microhardness. This enhancement in microhardness was observed due to quenching and pinning effects. However, for groove width exceeding 3 mm, a reduction in microhardness was observed. An increase in groove width indicates an increase in the volume of reinforcement particles and this increase in volume tends to reduce the inter-particle spacing. Also with the increase in groove width, the formation of voids and other defects were observed and due to the same resulting composites were characterized by lower microhardness. Thus, the optimum ratio of groove width to tool shoulder diameter was 0.5. By maintaining this ratio, enhanced mechanical properties along with homogenous distribution of reinforcement particles was observed. Rahsepar and Jarahimoghadam (2016) performed multi-pass FSP on AA 5052/$ZrSiO_4$ and investigated the consequence of the same on corrosion behavior and mechanical properties. It was observed that multi-pass FSP tends to improve the distribution of reinforcement particles along with the refinement of grain

size. It was also reported that corrosion resistance improves with an increase in the number of passes from one to three. However, an increase in number of passes beyond three results in the reduction of corrosion resistance. It was reported that enhancement in mechanical properties was attributed to pinning effect and quenching.

Dadashpour et al. (2016) fabricated AZ91C/SiO_2 surface composite using FSP. It was reported that Hall-Petch and Orowan effects were the dominating mechanisms for improvement in tensile strength and hardness. With the increase in the number of passes, a reduction in the agglomeration of SiO_2 particles were observed. Lack of distribution and aggregation of reinforcing particles in the matrix were found to support the cavity formation. These cavities were found to transform into initial cracks and will result in weak bonding. Due to the same, specimen fabricated using a single pass was found to have lower fractural toughness when compared to specimen fabricated using 3 passes. It was observed that the addition of SiO_2 particles in the magnesium matrix creates stress concentration at the interface of matrix and reinforcement. This stress concentration will reduce the toughness of resulting composites. Jamshidijam et al. (2013) observed improvement in mechanical properties owing to homogenous distribution of multiwall C in magnesium matrix. Compared to magnesium alloys, the grain size was found to reduce to 0.5 μm post FSP. Due to this grain reduction and high interfacial strength, improvement in microhardness of resulting surface composite was observed. The wear resistance of the resulting surface composite was twice the wear resistance of base alloys. This improvement was attributed to a lower coefficient of friction and higher hardness. Bhadouria et al. (2017) performed FSP in normal and underwater conditions and investigated the resulting microstructure and tribological properties. Optimum parameters were rotational speed of 1000 rpm, transverse speed of 50 mm/min with 6 numbers of passes. While comparing microstructure, it was observed that immersed FSP specimens were having higher grain reduction compared to air FSP specimens. Similarly, higher microhardness and wear resistance were observed for immersed FSP specimens. This improvement was accredited to the removal of excess friction heat and dynamic recrystallization which will lead to post grain grown in immersed FSP specimens. Thankachan Prakash and Kavimani (2018a) fabricated copper based surface composites reinforced with 5, 10 and 15% boron nitride (BN). With the increase in volume percent of reinforcement particles, mechanical and tribological properties were found to improve significantly. Thankachan Prakash and Kavimani (2018b) investigated the microstructure

and mechanical properties of the copper based surface composite. Similar to other researches, fine reinforcement particles were homogeneously distributed on the surface of the copper matrix. However, with an increase in the content of reinforcement particles, a reduction in ductility and corrosion rate was observed.

2.3 Friction Stir Welding of Aluminium Matrix Composites

Existing literature in the area of Friction Stir Welding (FSW) of MMC was referred and critically reviewed. The review of macrostructure, microstructure, joint properties such as tensile strength, hardness, wear and corrosion, residual stresses and wear of FSW tool will be discussed in subsequent sections.

2.3.1 Macrostructure of Welded Joint

Investigating the macrostructure and microstructure reveals the quality of the weld joint. Welding parameters such as welding speed, rotational speed, axial load, tool design and tool tilt angle dominates the resulting macrostructure and microstructure of weld joint. The rotating tool generates frictional heat due to which the workpiece is subjected to several thermal cycles. During these thermal cycles, workpiece material deforms plastically at the higher temperature. Depending upon the friction between tool and workpiece, insufficient or excessive heat will be generated which results in the formation of defects such as tunnel defects, voids, insufficient material flow, kissing bond, etc. The generated heat also affects the shape and structure of various zones. Thus to avoid these defects, a proper range of process parameters must be selected. Microstructure evaluation of various pilot experiments helps in selecting the working range of process parameters. Thus, evaluation of macrostructure and microstructure is extensively essential.

As discussed earlier, the macrostructure reveals four different zones: Weld or Nugget Zone (NZ), Thermomechanically Affected Zone (TMAZ), Heat Affected Zone (HAZ) and Base Metal (BM). The various zones observed in welded MMC is shown in Figure 2.12. The conditions such as type of base metal, the thickness of the workpiece, process parameters, design of the tool and many more, significantly affect the macrostructure of the weld joint. Two distinct shapes of NZ i.e. basin shape and elliptical shape was observed (Mishra & Ma, 2005). Both types of profiles are shown in Figure 2.13. While performing FSW of AA 2009 /15% SiC composites, NZ was found to have an elliptical shape (Feng, Xiao, & Ma, 2008). Macrostructure of as-weld specimens was

compared with post-weld heat treated samples and no subsequent change in macrostructure was observed. On the other side, AA 2009-T351 + SiC composite was found to have a basin profile of NZ (Ni, Chen, Wang, Xiao, & Ma, 2013). However, FSW of AA 7075-O was found to have basin shape of NZ while for AA 7075 reinforced with nano-sized SiC particles, an elliptical shape of NZ was observed (Bahrami, Nikoo, & Givi, 2014).

While observing the macrostructure of Al + Mg_2Si and A356 + SiC composites, it was observed that HAZ was not visible in the macrostructure. As these composites are lesser sensitive to thermal variation, HAZ was not clearly visible (Nami, Adgi, Sharifitabar, & Shamabadi, 2011; Amirizad, et al., 2006). Another feature that characterizes the macrostructure of the weld joint is the visibility/invisibility of the onion ring structure. As shown in Figure 2.14, FSW of AA6061/Al_2O_3 was found to have an onion ring structure. It was reported that visibility/invisibility of onion ring structure depends upon the flow of plasticized material (Ceschini, Boromei, Minak, Morri, & Tarterini, 2007b). Apart from this, it should be noted that the dislocation density caused during the welding process results in the formation of an onion ring structure. FSW of AA 6063/B_4C reported that the onion ring structure was invisible due to partial recrystallization which occurred as a result of improper heat generation (Chen, Silva, Gougeon, & St-Georges, 2009). While observing the effect of various tool pin profiles on welded AA 7075/SiC, complete onion ring structure was only visible for the joints welded using threaded tapered pin (Bahrami, Givi, Dehghani, & Parvin, 2014). Whereas, joints welded using other tool pin profiles were having either partial onion ring structure or onion ring structure was invisible. This indeed indicates generation of insufficient heat and partial recrystallization. Nami et al. (2011) performed FSW of aluminium alloy reinforced with magnesium silicate (Mg_2Si). They examined the variation in microstructure by changing the number of passes. While increasing the number of passes, the formation of defects in the NZ was found to increase. The formation of the defect was either due to improper material flow or due to excessive/lack of heat input.

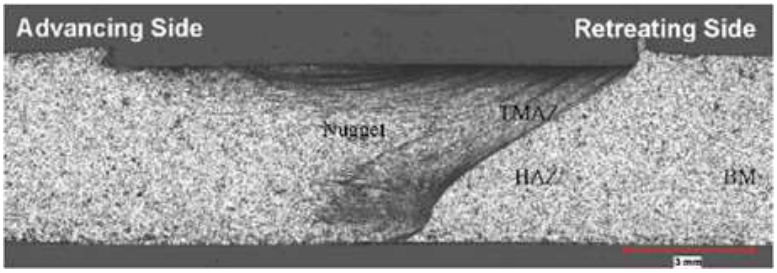

Figure 2.12 Macrostructure of FSWed AA 6061 + 10% B_4C with four distinct zones (Chen, Silva, Gougeon, & St-Georges, 2009)

Figure 2.13 Profile of NZ (a) Basin and (b) Elliptical (Mishra & Ma, 2005)

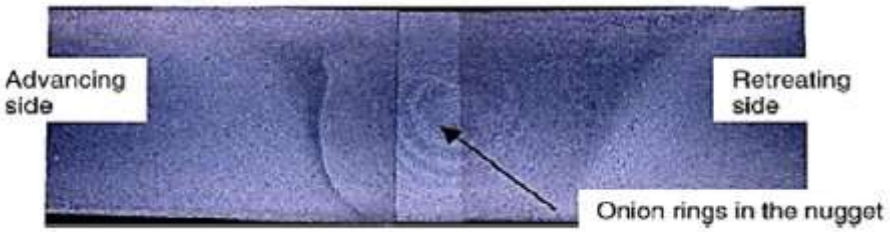

Figure 2.14 Onion ring structure in NZ (Ceschini, Boromei, Minak, Morri, & Tarterini, 2007b)

2.3.2 Microstructure of Welded Joint

Distribution of Reinforcement Particles

During the FSW process, the heat generated will be approximately 80% of the melting temperature of MMC. Due to this, the material will undergo recrystallization. During the manufacturing of MMC, the reinforcement particles are either heterogeneously distributed or form clusters in the matrix. The rotating tool generates stirring action which ultimately leads to refinement of reinforcement particles. Not only this, the rotating tool will also result in homogenously distributes these particles in NZ. Also, the rotating tool tends to break the clusters present in base composites (Chen, Silva, Gougeon, & St-Georges, 2009; Amirizad, et al., 2006) and thus results in homogenous distribution of reinforcement particles (Bozkurt, Uzun, & Salman, 2011; Bahrami, Givi,

Dehghani, & Parvin, 2014; Uzun, 2007; Dinaharan & Murugan, 2012).

However, along with the homogenous distribution, the microstructure was also characterized by the presence of a cluster of reinforcement particles. It has been reported that the distribution of nano-reinforcement particles during FSW was found to be critical (Simar & Avettand-Fenoel, 2016). Some heterogeneity was also observed when elongated reinforcement particles were aligned with the sense of material flow (Mertens, et al., 2015; Storjohann, et al., 2005). During FSW of Al/SiC composites, it was observed that in TMAZ the alignment of SiC whiskers was along the direction of material flow. The same has been shown in Figure 2.15. The distribution of SiC whiskers in the NZ was similar to that of the base composite. However, the orientation of those SiC whiskers in NZ was found to have varied from top to bottom surface of the weld joint. Apart from this, inhomogeneous distribution of reinforcement particles was reported when offset was provided to the workpiece. It was observed that the advancing side was having a lower weight percent of SiC particles compared to retracting side (Xiao, Wang, Bi, Zhang, & Ma, 2010).

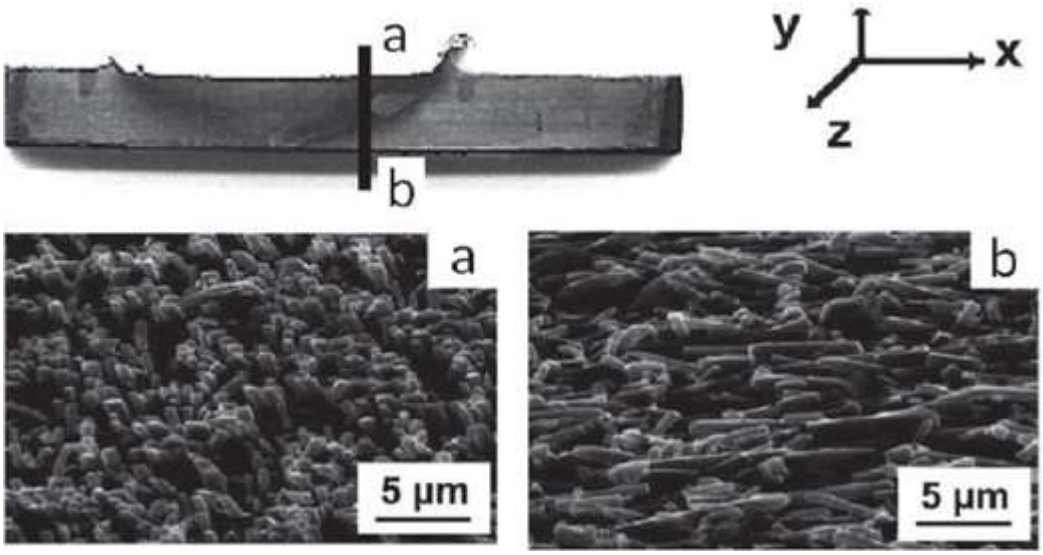

Figure 2.15 Distribution of SiC particles in FSWed AMC (a) at top of NZ and (b) at the bottom surface of NZ near TMAZ (Storjohann, et al., 2005)

It should be noted that no subsequent change in microstructure was observed with the variation in rotational speed and welding speed (Cioffi, et al., 2013; Yabuuchi, et al., 2014). However, higher welding speed caused the insufficient flow of material and due to the same, agglomeration of SiC particles was reported. During FSP it was observed that

reinforcement particles tend to distribute more homogenously with the subsequent number of passes (Simar & Avettand-Fenoel, 2016). However, it should be taken into consideration that during FSW, the rotating tool tends to generate an asymmetric flow of material on the advancing and retreating sides. Thus, to obtain the more homogenous distribution of reinforcement particles with multi-pass welding, during each new pass the advancing sides can be inverted (Azizieh, Kokabi, & Abachi, 2011; Lee, Huang, & Hsieh, 2006; Mahmoud, Takahashi, Shibayanagi, & Ikeuchi, 2010). Considering three different pin profiles i.e. taper octagon, taper square and taper hexagon, it was observed that joint fabricated using taper square pin profile was found to have a more homogenous distribution of reinforcement particles (Kalaiselvan & Murugan, 2012; Gopalakrishnan & Murugan, 2011).

Size and Shape of Reinforcement Particles

In the available literature, refinement of reinforcement particles in NZ when compared to base composite have been reported (Marzoli, Strombeck, Dos Santos, Gambaro, & Volpone, 2006; Murugan & Kumar, 2013; Kumar, Mahapatra, Jha, Mandal, & Devuri, 2014; Yigezu, Venkateswarlu, Mahapatra, Jha, & Mandal, 2014). The abrasion between tool and reinforcement particles along with the stirring action reduces the aspect ratio of reinforcement particles. The literature also reports that the edges of reinforcement particles were rounded or blunt along with the reduction in shape factor (Ni, Chen, Xiao, Wang, & Ma, 2013; Kumar, Nayak, Herbert, & Rao, 2014). However, it was observed that refinement of the reinforcement particles can be obtained using a tool having a smooth pin (Fernandez & Murr, 2004). Apart from these, literature reported the presence of a spherical Mg_2Si needle like structure, which leads to minimization of surface energy. It was observed that no dissolution of reinforcement particles occurs during the welding process. Due to the refinement of reinforcement particles, improvement in mechanical properties was observed. Storjohann et al. (2005) reported that while taking the finer size of reinforcement during the welding process, the particles will not be subjected to further refinement.

Some researchers report coarsening of the reinforcement particles in the NZ (Wang, Yuan, Mishra, & Charit, 2013; Mathon, Klosek, Carlan, & Forest, 2009). It was reported that coarsening of reinforcement particles had occurred due to phase transformation and reaction between the matrix and reinforcement particles during FSW. From Figure 2.16 it

can be observed that, due to good chemical affinity and coalescence, Y_2O_3 was found to have agglomeration with Ti and Al. However, during FSW of ODS steel, minor coarsening of the oxides reinforcement present in the NZ was observed. Along with this, a reduction in density of the reinforcement particles was also reported (Yabuuchi, et al., 2014). As a result of coarsening, a reduction in mechanical properties of welded joints was observed. Also due to inadequate heat generation, larger grain size along with aggregated reinforcement particles in NZ was observed (Bahrami, Givi, Dehghani, & Parvin, 2014). Feng et al. (2008) compared the shapes of SiC particles and reported that the reinforcement particles present in the NZ were slightly blunt and some of the particles were found to have micro-cracks. The average size of reinforcement particles was found to decrease from 5.4 µm in the based composite to 4.2 µm in the NZ. Marzoli et al. (2006) reported that NZ was characterized with refined particles having a circular shape, which was absent in the base composite.

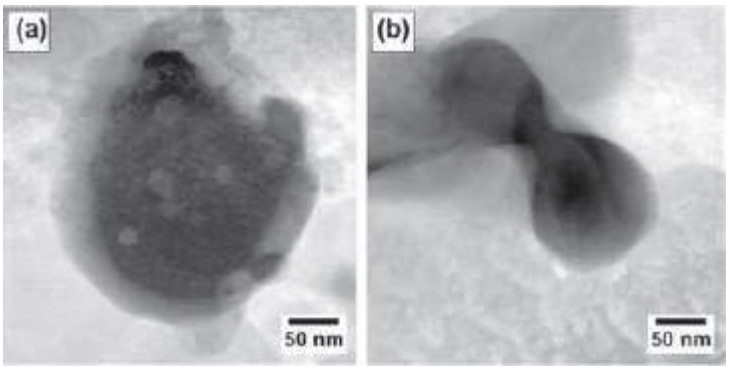

Figure 2.16 FSW of an oxide-dispersion-strengthened MA754 Ni based alloy: (a) agglomeration particle and (b) formation of the neck between two Y_2O_3 dispersoids (Feng, Xiao, & Ma, 2008)

Effect of Other Parameters on Microstructure

Owing to dynamic recrystallization, it was observed that new grains had nucleated in the NZ. As a result of this, the NZ was characterized by equiaxed grains. These equiaxed grains were found to have a smaller grain size when compared to base composite. Feng et al. (2008) examined the change in microstructure under influence of Post Weld Heat Treatment (PWHT). Before PWHT, NZ was found to have fine equiaxed recrystallized SiC particles with a grain size of 5 µm. After PWHT, grain growth in the nugget zone was observed and grain size was increased to 8 µm. While evaluating the consequence of pin profile on microstructure, the use of square pin was suggested for obtaining smaller

and finer grain structure (Hassan, Qasim, & Ghaithan, 2012). Bozkurt et al. (2011) compared the microstructure of various zones and it was observed that the microstructure of HAZ was more or less analogous to that of base composite. Comparatively higher heat is generated in TMAZ and NZ will result in the generation of higher stress. Due to this high stress, both the aforementioned zones were subjected to rearrangement of particles. Ceschini et al. (2007) while examining variation in the area of reinforcement particles, a reduction in the area of particles located near the tool shoulder was repoerted. The area of particles located near the tool shoulder was reduced by 60%, compared to particles in the base composite.

2.3.3 Tensile Strength

The factors such as manufacturing methods, types of ceramics particles, the weight percent of ceramic particles and range of process parameters, which governs the tensile properties. The Ultimate Tensile Strength (UTS), yield stress, elongation, joint efficiency and process parameters of various welded MMC are shown in Table 2.1. The addition of ceramic particles to alloys improves the tensile properties of alloys. Existing literature reports that MMC joined using the FSW process exhibits higher tensile strength compared to the joint fabricated using the conventional welding process. Overall improvement in mechanical properties such as hardness, elastic modulus, ultimate tensile strength, elongation and yield strength was observed (Dragatogiannis, Koumoulos, Kartsonakis, Pantelis, & Charitidis, 2016; Pantelis, et al., 2015). Bozkurt et al. (2011) showed that welded specimens had failed either from base metal or from HAZ, indicating higher tensile strength of NZ compared to others zones. When compared to the base composite, a reduction of 19% in tensile strength of NZ was observed. Ceschini et al. (2007b) for FSW of AA 6061/20% Al_2O_3 reported a reduction of 28% in tensile strength of weld joint compared to base composite. Ceschini et al. (2007a) in their another study on FSW of AA 7005/10% Al_2O_3 observed a reduction in tensile strength and joint efficiency by 20% and 80% respectively, when compared to base composites. On the other side, Amirizad et al. (2006) compared various tensile properties of base composite and welded composites. They observed higher tensile properties of weld joints compared to base composite. There were two reasons for the improvement in the tensile properties of the weld joint i.e. (i) homogenously distributed ceramic particles and (ii) reduction in defects.

Table 2.1 Ultimate Tensile Strength (UTS), yield stress, elongation, joint efficiency and process parameters of various welded MMC (cont.)

Sr. No.	Workpiece Material	Processing	Material Thickness (mm)	Welding Speed (mm/min)	Rotational Speed (rpm)	Ultimate Tensile Strength (MPa)	Yield Stress (MPa)	Elongation (%)	Joint Efficiency (%)	Reference
1	AA 6061/10% ZrB_2	Casting	6	48.8	1155	243	-	-	95.8	(Dinaharan & Murugan, 2012(a))
2	MA956 steel/0.053% Y_2O_3	Hot Rolling + Annealing	3.4	51	1000	736	574	30.7	124	(Wang, Yuan, Mishra, & Charit, 2013(a))
3	AA 6061/12% B_4C	Casting	6	78	997	208	-	-	96.83	(Kalaiselvan & Murugan, 2013)
4	MA754, Ni-19.54Cr-0.27Al-0.46Ti + 0.64% Y_2O_3	Hot Rolling + Annealing	-	50.8	1000	970	648	27	96	(Wang, Yuan, Mishra, & Charit, 2013)
5	AA 6061/12% B_4C	Casting	6	80	1000	201	-	2.5	93.4	(Kalaiselvan, Dinaharan, & Murugan, 2014)
6	High Cr-ODS steel + 0.34 %Y_2O_3	Powder Metallurgy + Hot Rolling	1.5	-	250	980	-	15	83	(Yabuuchi, et al., 2014)
7	AA 6061/AlN	Casting	6	55	1200	225	-	0.77	93.42	(Kumar & Murugan, 2014)
8	Al/10% TiB_2	Casting	6	30	2000	223-282	-	3.4-6.7	79-99	(Vijay & Murugan, 2010)
9	AA 7075/10% Al_2O_3	Extruded-T6	7	56	800	260	245	0.58	83.87	(Cavaliere, Cerri, Marzoli, & Dos Santos,

Table 2.1 Ultimate Tensile Strength (UTS), yield stress, elongation, joint efficiency and process parameters of various welded MMC (cont.)

Sr. No.	Workpiece Material	Processing	Material Thickness (mm)	Welding Speed (mm/min)	Rotational Speed (rpm)	Ultimate Tensile Strength (MPa)	Yield Stress (MPa)	Elongation (%)	Joint Efficiency (%)	Reference
										2004)
10	AA 6061/20%Al_2O_3	Extruded-T6	7	56	800	329	280	1.3	86.8	(Cavaliere, Cerri, Marzoli, & Dos Santos, 2004)
11	Al + 4.5% Cu + 10%TiC	Casting + Hot Rolling	8	20	500	172	-	2.83	-	(Kumar, Mahapatra, Jha, Mandal, & Devuri, 2014)
12	AA 6061/20%Al_2O_3	Extruded-T6	7	300	700	251	234	-	70	(Marzoli, Strombeck, Dos Santos, Gambaro, & Volpone, 2006)
13	Al + 12% SiC + 10% SiC	Casting + Hot Rolling	8	20	500	175	-		2.28	(Yigezu, Venkateswarlu, Mahapatra, Jha, & Mandal, 2014)
14	Al + 15% Mg_2Si	Gravity Casting	6	125	1120	115	-	-	-	(Nami, Adgi, Sharifitabar, & Shamabadi, 2011)
15	AA 6061/22% Al_2O_3	Casting	4	260	880	227	-	-	99	(Minak, Ceschini, Boromei, & Ponte, 2010)

Table 2.1 Ultimate Tensile Strength (UTS), yield stress, elongation, joint efficiency and process parameters of various welded MMC (cont.)

Sr. No.	Workpiece Material	Processing	Material Thickness (mm)	Welding Speed (mm/min)	Rotational Speed (rpm)	Ultimate Tensile Strength (MPa)	Yield Stress (MPa)	Elongation (%)	Joint Efficiency (%)	Reference
16	$AlMg_5$ + 0.5% Al_2O_3 (nano-particles)	Powder Metallurgy	6.5	60	600	397	262	15.5	82	(Babu, et al., 2016)
17	AA 606/ 10%SiC	Casting	6	45	1100	206	126	6.5	74	(Periyasamy, Mohan, & Balasubramanian, 2012)
18	AA2124-T6 + 25 SiC	Powder Metallurgy	15	75	550	642.1	478	2.9	86	(Cioffi, et al., 2013)
19	AA 6061/ 10%SiC	Casting	6	88.9	1370	265	-	-	92.3	(Periyasamy, Mohan, Balasubramanian, Rajakumar, & Venugopal, 2013)
20	Al AC4A + 30% SiC	-	5	150	2000	140	-	0.33	86	(Liu, Hu, Zhao, & Fujii, 2015)
21	AA 2124 + 25% SiC	Forged T4	3	40	1120	366	-	-	81	(Bozkurt, Kentli, Uzun, & Salman, 2012)
22	Al alloy LM 25 + 5% SiC	Stir Casting	6	20	1200	95.1	-	-	-	(Devanathan & Babu, 2014)
23	AA 2009 + 15% SiC	Extruded-T4	8	50	600	450	320	3	95	(Feng, Xiao, & Ma, 2008)
24	AA 6061 + 12% AlN	Stir Casting	6	55	1200	210	-	-	93	(Murugan & Kumar, 2013)

Table 2.1 Ultimate Tensile Strength (UTS), yield stress, elongation, joint efficiency and process parameters of various welded MMC (cont.)

Sr. No.	Workpiece Material	Processing	Material Thickness (mm)	Welding Speed (mm/min)	Rotational Speed (rpm)	Ultimate Tensile Strength (MPa)	Yield Stress (MPa)	Elongation (%)	Joint Efficiency (%)	Reference
25	AA 6061 + 10% ZrB_2	Casting	6	50	1150	240	-	1	95	(Dinaharan & Murugan, 2012)
26	AA 6063 + 10.5% B_4C	Extrusion	4.5	600	1500	172	136	2.4	49	(Chen, Silva, Gougeon, & St-Georges, 2009)
27	AA 7075-T6 + 10% Al_2O_3	Casting + Extrusion	7	300	600	299	260	1.3	80	(Ceschini, Boromei, Minak, Morri, & Tarterini, 2007a)
28	AA 2009-T4 + 15% SiC	Powder Metallurgy + Hot Rolling	6	100	800	559	331	11.4	104	(Wang, Xiao, Wang, & Ma, 2014)
29	AA 2009-T4 + 15% SiC	Powder Metallurgy + Hot Rolling	6	100	800	521	334	7.1	95	(Wang, Xiao, Wang, & Ma, 2013)
30	AA 2009 + 17% SiC	Extruded T4	3	800	1000	501	341	3.5	97	(Wang, Wang, Xiao, & Ma, 2014)

Response of Process Parameter on Tensile Strength and Percentage Elongation

Kumar et al. (2004) performed FSW on AA 6061/AlN and examined the consequence of welding parameters on tensile strength along with elongation. They reported that for the rise in rotational speed upto 1200 rpm, tensile strength improves. However, increase in rotational speed beyond 1200 rpm tends to reduces the tensile strength. Change in tensile strength with the variation in welding speed and axial load was found to have a similar trend. Maximum tensile strength was observed for the joint which was welded by maintaining a welding speed of 55 mm/min. Maximum tensile strength was obtained for 5 kN of axial load. However, percentage elongation was found to have a direct proportion with welding speed and inverse proportion with rotational speed and axial load. It was observed that the rise in weight percent of reinforcement particles, appreciably improves the tensile properties of the welded joints. Yigezu et al. (2014) for FSW of aluminium reinforced with 12% of Si and 10% of TiC, explored the consequence of process parameters. The increase in rotational speed (from 710 rpm to 1000 rpm) and transverse speed (from 20 mm/min to 40 mm/min) was found to have an adverse effect on tensile strength and elongation. On the other side, improvement in both properties was observed when shoulder diameter was varied from 18 mm to 20 mm. However, a further increase in shoulder diameters results in a drop of both properties.

Kumar et al. (2014) for FSW of aluminium reinforced with 4.5% Cu/TiC, reported a reduction in tensile strength when welding was performed with varying rotational speed (from 500 rpm to 710 rpm) and welding speed (from 20 to 40 mm/min). Based on the nature of contact between tool and workpiece three different profiles of pins were designed. Maximum tensile strength was observed for the sample which was fabricated using a tool having maximum contact with the workpiece. Among various tool designs i.e. cylindrical pin, taper pin and threaded taper pin, maximum tensile strength was obtained for threaded taper pin (Shah, Goyal, & Patel, 2015). Wang et al. (2014) joined AA 2009 reinforced with 15% SiC using the FSW process. Experiments were performed by maintaining a constant rotational speed of 1000 rpm and varying welding speed in the range of 50 mm/min to 800 mm/min. The specimen welded by maintaining a welding speed of 800 mm/min was found to have higher tensile strength compared to other specimens. Nami et al. (2011) observed that increasing the rotational speed upto 1120 rpm improves the tensile strength. However, an increase in rotational speed beyond 1120

rpm reduces the tensile strength. Also, it was observed that tensile strength tends to reduce, with an increase in the number of passes. Chen et al. (2009) reported that failure of the welded joint had either occurred from NZ or from TMAZ on advancing side. As an effect of artificial ageing, significant improvement in tensile strength and joint efficiency was observed.

Dinaharan et al. (2012) examined the consequence of the increase in volume percent of reinforcement particles. It was found that tensile strength was having direct proportion with the increase in volume percent of reinforcement particles. On the other hand, percentage elongation was found to have an inverse relation with the increase in volume percent of reinforcement particles. It was observed that unreinforced specimens were having joint efficiency of 99% whereas, reinforced specimens were found to have 95%. A similar trend was reported by other researchers (Bahrami, Dehghani, & Givi, 2014; Kalaiselvan, Dinaharan, & Murugan, 2014). Xiao et al. (2010) evaluated the changes in tensile strength by providing tool offset. They reported that due to aggregation of the Al layer on the retreating side, the samples with offset showed lower tensile strength when compared to sample without offset. Due to offset, the tensile strength was found to reduce from 85% to 47%.

Response of Tool Pin Profile on Tensile Strength

Bahrami et al. (2014) considered several pin profiles such as triangular, square, threaded tapered, four flutes cylindrical and four flute square. They examined the consequence of these pin profiles on resulting tensile strength of weld joint. Among various profiles of the pin, maximum tensile strength was obtained by using a triangular pin. On the other side, minimum tensile strength was observed for a four flutes cylindrical profile of the pin. Vijay et al. (2010) for FSW of Al/TiB_2, considered different pin profiles such as taper square pin, straight square pin, taper hexagonal pin, straight hexagonal pin, taper octagonal pin and straight octagonal pin. Among all these profiles, maximum tensile strength was obtained for the straight square pin and minimum tensile strength was observed for the taper square pin. Due to the presence of TiB_2 particles, the effect of pin profile on elongation was negligible. Similarly, Hassan et al. (2012) also reported that among various profiles of the pin, maximum tensile strength was obtained using a square pin profile.

Effect of Post Weld Heat Treatment on Tensile Strength

Feng et al. (2008) observed the consequence of Post Weld Heat Treatment (PWHT) on tensile strength. It was reported the application of PWHT can significantly enhance the tensile strength. However, it was also observed that the hike in tensile strength of the base composite was much higher than that of welded joint. The detailed investigation showed that after PWHT, the weld zone was characterized by the Cu_2FeAl_7 phase due to which, a reduction in tensile strength was observed. Wang et al. (2013) for FSW of AA 2009/15% SiC reported that during T4 tempering, complete dissolution of Al_2Cu phase had occurred. This ultimately improved the tensile strength of the welded joint.

2.3.4 The Hardness of Welded Joint

Hardness is measured perpendicular to the welding direction so that the change in hardness for various zones of the weld joint can be obtained. Two types of hardness profiles have been reported by various researchers. In the first profile, the highest hardness was observed in NZ, which tends to decrease in transition zone and reduces until the hardness of base composite (Shettigar, Salian, Herbert, & Rao, 2013; Feng, Xiao, & Ma, 2008; Nami, Adgi, Sharifitabar, & Shamabadi, 2011; Amirizad, et al., 2006) Similar profile is shown in Figure 2.17. This occurs due to the presence of refined and homogeneously distributed reinforcement particles in NZ. Nami et al. (2011) also made a similar observation and recorded significantly higher hardness in NZ compared to base composite. They also reported that with an increasing number of passes, the hardness of the weld joint decreases. Feng et al. (2008) reported that maximum hardness was obtained in NZ. Due to PWHT, improvement in hardness of all zones was observed. However, the improvement in hardness of NZ was considerably low compared to other zones. Wang et al. (2013) reported hardness of 150 HV in the nugget zone which was comparatively higher than the base metal. After T4 conditioning, welded sample revealed a uniform hardness of approximately 170 HV.

The second type of hardness profile is the “W” shape profile, which is shown in Figure 2.18. Similar profile has been reported by many researchers (Ni, Chen, Wang, Xiao, & Ma, 2013; Bozkurt, Uzun, & Salman, 2011; Ceschini, Boromei, Minak, Morri, & Tarterini, 2007a; Marzoli, Strombeck, Dos Santos, Gambaro, & Volpone, 2006; Kalaiselvan & Murugan, 2013). In this type of profile, base composite will have the

highest hardness, which decreases through TMAZ upto HAZ and then it again increases in NZ. Normally, NZ has lower hardness compared to base composite. Bozkurt et al. (2011) reported that the hardness of the upper side of weld joint was comparatively lower than the hardness of the lower side. A well-known fact implies that some dislocation will always be generated due to the difference in thermal expansion of reinforcement particles and matrix. This difference will be more in NZ compared to HAZ. Thus, HAZ will have the lowest hardness compared to other zones. Uzun et al. (2007) for FSW of AA 2124/SiC observed that HAZ was characterized by minimum hardness which was found to improve gradually in TMAZ and NZ. When compared to the hardness of NZ, a negligible improvement in the hardness of the base composite was observed.

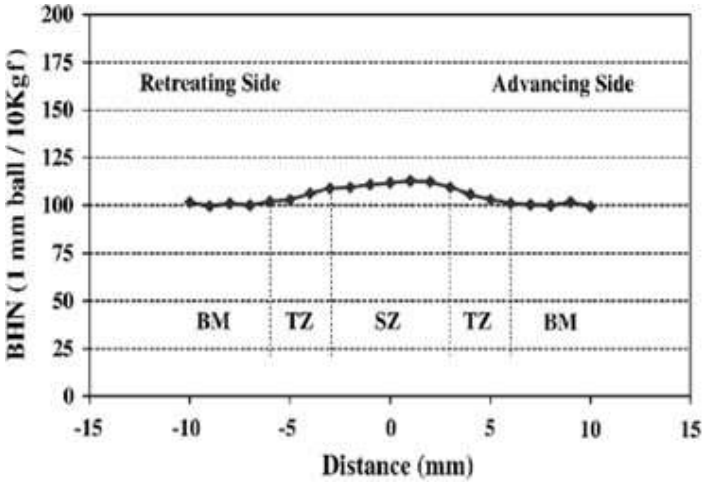

Figure 2.17 Hardness profile for A356 + 15% SiC (Amirizad, et al., 2006)

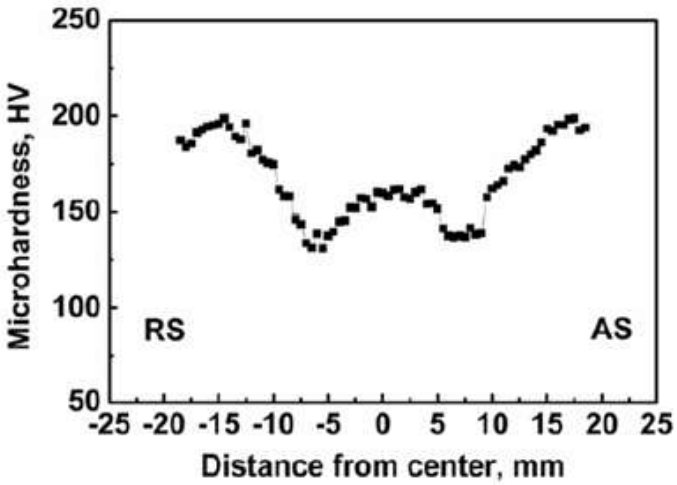

Figure 2.18 Microhardness profile for FSW of AA 2009 + SiC (Ni, Chen, Wang, Xiao, & Ma, 2013)

However, few researchers observed a reduction in hardness while moving from TMAZ to NZ (Ceschini, Boromei, Minak, Morri, & Tarterini, 2007a; Ceschini, Boromei, Minak, Morri, & Tarterini, 2007b). Chen et al. (2009) while comparing the hardness of reinforced and unreinforced specimens found that there was no considerable difference in hardness due to the addition of B_4C. In the contrast, Bahrami et al. (2014) observed higher hardness of unreinforced joints compared to reinforced joints. Dinaharan et al. (2012) found that the hardness of weld joints was improving with the increase in volume percent of reinforcement particles. Xiao et al. (2010) observed that by providing offset, the hardness of NZ on the retreating side was having the maximum value. Whereas, HAZ on the advancing side was found to have a minimum value of hardness.

Yigezu et al. (2014) observed that an increase in rotational speed leads to improve the hardness. The same trend was also obtained with increasing shoulder diameter whereas, the increasing nature of welding speed was found to have a reverse trend. Wang et al. (2014) observed that HAZ was found to have two zones with the lowest hardness when welding speed was maintained at 50 mm/min. An increase in welding speed to 200 mm/min, improves the overall hardness of welded joint but it also retains those two zones with the lowest hardness. Performing welding at 800 mm/min it was observed that the lowest hardness was present in NZ and two zones (with lower hardness) present in HAZ was reduced to one. Bahrami et al. (2014) considered various profiles of the pin and obtained maximum hardness for welded joint fabricated using the four flutes cylindrical profile of the pin. While investigating the effect of the number of passes on microhardness distribution, no considerable improvement in hardness was reported. However, reduction in variation in microhardness was observed for the double pass (Ahn, Choi, Kim, & Jung, 2012).

2.3.5 Wear Properties and Corrosive Properties of Welded Joint

The addition of reinforcement particles improves the wear resistance of material as it ultimately improves hardness. Dinaharan et al. (2012) examined the wear properties of FSWed AA 6061/ [0, 5 and 10%] ZrB_2. With the increase in weight percent of ZrB_2 particles, it was observed that the wear rate of weld joint reduces. The worn surfaces of both welded and as-cast composites were found to have high plastic deformation. The plastic deformation during the joining process reduces when the composite is reinforced with a higher weight percent of particles. For as-cast AA 6061 and AA 6061 + 5% ZrB_2,

adhesive wear behavior was observed, whereas 10% of ZrB_2 showed abrasive wear behavior. Similarly, 3 times higher wear loss in base composite compared to NZ was also reported (Lee, Kim, Yoon, Kim, & Yoen, 2006). Lee et al. (2006) reported a difference of 25% in wear rate i.e. parent composite was found to have a higher wear rate compared to welded specimens. Hassan et al. (2012) examined the effect of process parameters on wear properties of the weld joint. They concluded that joints fabricated using square profiles were found to have the best wear resistance compared to joints fabricated using other profiles of the tool. For constant welding speed and square pin profile, an increase in rotational speed tends to reduce the wear resistance of the weld joint. This was supported by the fact that rising rotational speed will generate higher heat. Higher heat generation will lead to coarsen microstructure, which will ultimately reduce the wear resistance. With constant rotational speed and square pin profile, an increase in wear rate was observed with the increase in welding speed till 45 mm/min. With a further increase in welding speed, reduction in wear rate was observed. This nature of wear resistance was supported by the fact that higher welding speed will increase the cooling rate which ultimately refines the grain structure and increases the hardness and wear resistance of the welded joint.

2.4 Summary

A systematic and detailed literature review has been carried out. The literature review can be summarized as follows:

- It should be noted that the stir casting process is still under research phases and thus don't find much industrial applications. Several researchers and academicians are working on various aspects of the stir casting process with a prime focus on (i) analyzing microstructure, (ii) evaluating mechanical and tribological properties, (iii) consequence of process parameters and their optimization, (iv) machinability, (v) consequence of the size of secondary phase particles and many more. Apart from this, there exist several review articles which provide comprehensive information about the stir casting process for the manufacturing of MMC.

- There exists a variety of literature whose major concern was to obtain desire mechanical, tribological and corrosive properties along with homogenous

distribution of reinforcement particles in surface composites. Apart from this, the literature also reveals the effect and optimization of process parameters. Furthermore, there exist several review articles which elaborate several aspects of FSP such as strategies for obtaining the homogeneous distribution of the reinforcement particles, recent progress in the manufacturing of surface composite and optimization process parameters.

- The fusion welding of Metal Matrix Composites (MMC) supports a deleterious reaction between matrix and reinforcement particles. This reaction ultimately reduces the mechanical properties of the welded composites. Thus, to avoid this deleterious reaction, a solid state welding process such as Friction Stir Welding (FSW) process can be implemented. FSW has proven to be an appropriate option for the successful joining of MMC. It has been reported that joints fabricated using FSW exhibits higher mechanical properties compared to that fabricated using the fusion welding process.

- Depending upon the thermo-mechanical histories experienced during the welding process, the macrostructure of welded joint was found to have four different zones. The conditions such as type of base composite, the thickness of the workpiece, process parameters, design of the tool and many more significantly affect the macrostructure of the welded joint. Two distinct shapes of NZ have been reported: Basin Shape and Elliptical Shape. Another feature of macrostructure was the formation of the onion ring structure in NZ. The formation of the onion ring structure significantly depends upon flow of the plasticized material during the welding process. However, few researchers had reported that due to improper selection of process parameters defects such as voids, tunnel defects, kissing bond etc. were visible.

- As a result of the stirring action created by the rotating tool, the microstructure of the nugget zone was found to have a homogenous distribution of reinforcement particles. It was observed that the rotating action of the tool tends to breaks the clusters present in the base composites and thus leads to grain refinement. However, few of the researchers have observed a small agglomeration of the reinforcement particles in NZ. It was observed that due to the rotating tool, the edges of the reinforcement particles had become blunt or rounded.

- The presence of reinforcement particles in metal or alloy tends to improve the mechanical properties of alloys. With the same fact, it has been reported that the homogenous distribution of reinforcement particles increases the tensile strength of welded joints. Some of the researches have reported higher tensile strength of NZ compared to base composites. However, few have also states lower tensile strength of NZ compared to base composite. The hardness of the welded joint was found to have two types of profile. The first profile states that the NZ tends to have the highest hardness that decreases to the hardness of the base composite. The other profile of hardness was found to have a "W" shape indicating the highest hardness of base composites. Then the hardness decreases through HAZ to TMAZ and again increases in NZ. However, the hardness of the NZ will be comparatively lower than that of the base composite.

- Apart from these points, comparatively lower studies have been reported stating the effect of process parameters on mechanical properties of the welded joint. Few studies also reflect the effect of post weld heat treatment on microstructure and mechanical properties, tool wear during the welding process, the effect of tool pin profile and residual stress generated during the welding process.